Acta Cryst E
CRYSTALLOGRAPHIC COMMUNICATIONS

ISSN 2056-9890

Crystal structure of bis(diisopropylamino)fluoroborane

Tabea Lenz and Marian Hebenbrock*

University of Münster, Institute of Inorganic and Analytical Chemistry, Corrensstrasse 30, 48149 Münster, Germany. *Correspondence e-mail: hebenbro@uni-muenster.de

Received 14 February 2025
Accepted 8 April 2025

Edited by J. Reibenspies, Texas A & M University, USA

Keywords: crystal structure; fluoroborane,.

CCDC reference: 2441918

Supporting information: this article has supporting information at journals.iucr.org/e

The predominantly planar structure of a fluoro-substituted bis(dialkylamino)borane, $C_{12}H_{28}BFN_2$, was obtained from the reaction of boron trifluoride diethyl etherate with lithium diisopropylamide and its structure is presented here. While the B—F bond length is in the typical range of single B—F bonds, the B—N bond length indicates a partial double-bond character. The sterically demanding isopropyl groups on both amides increase the N—B—N angle and enable intermolecular van der Waals interactions.

1. Chemical context

Bis(dialkylamino)boranes and their derivatives have emerged as prominent starting materials in the field of boron chemistry due to their ease of functionalization and enhanced stability, attributable to the double-bond character of the B—N bond. The fact that these substituents can also be used to realize unusual coordination patterns on the B atom was first demonstrated in 1982 by Nöth and Parry through the formation of the two-coordinate borinium cation (Nöth *et al.*, 1982; Higashi *et al.*, 1982). Nöth generated the borinium cations from bis(dialkylamino)bromoboranes by reaction with Lewis acids, while Parry used analogous chloroboranes. This pioneering work was further expanded, exploring the use of a variety of amines, Lewis acids and boranes (Nöth *et al.*, 1984, 1986; Kölle *et al.*, 1986). More recently, Major *et al.* (2019) have demonstrated an alternative approach based on analogous fluorinated compounds, wherein a silylium cation functions as a fluoride abstractor. They also showed that these borinium cations are versatile reagents in hyroboration reactions. Here we report the structure of the starting material, bis(diisopropylamino)fluoroborane, **1**, which was also previously identified as a product of reactions of (diisopropylamino)difluoroboranes in the presence of Na/K alloy (Maringgele *et al.*, 1992, 1993), but its structure was never elucidated. The structural investigation of such a simple compound will contribute to the understanding of the basic binding situation and properties, and will provide a more complete picture when compared with analogous structures.

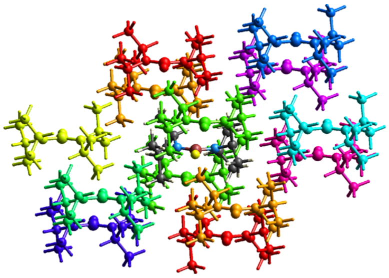

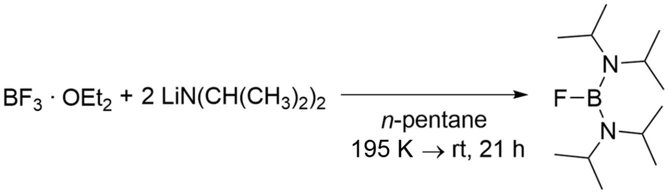

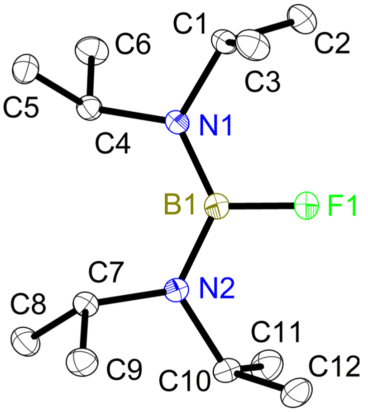

Figure 1
The asymmetric unit of the solid-state structure of compound **1**, with the atom-labelling scheme. Displacement ellipsoids are shown at the 50% probability level and H atoms have been omitted for clarity.

2. Structural commentary

Compound **1** crystallizes in the triclinic space group $P\overline{1}$ and has one molecule in the asymmetric unit (Fig. 1). The bond length between boron and fluorine [1.3650 (9) Å] falls within the typical range of bond lengths observed for B—F bonds. The B—N bond lengths [1.4227 (10) and 1.4206 (10) Å] not only correspond to typical boron alkylamides, but also show a bond length resulting from the partial formation of a B—N double bond. The N—B—N angle [128.91 (7)°] exhibits a slight increase compared to analogous compounds. This is attributed to the sterically demanding substituents present on both amines, along with the fluorine substituent, which exhibits a smaller steric bulkiness, thereby enabling the widening of the bond angle. The overall structure of the compound is predominantly planar, which is consistent with the expected geometry of a trigonal-substituted B atom with partial double bonds to the substituents.

3. Supramolecular features

Compound **1** does not show any significant intermolecular interactions. The formation of four-membered rings, as found for example in analogous aminoboron difluorides (Hazell, 1966; Edwards *et al.*, 1970; Jones, 1984), is not possible in the case of compound **1** due to the steric demand of the isopropyl side groups. The isopropyl groups themselves are capable of significant van der Waals interactions. These interactions were evaluated using the *CrystalExplorer* program (Spackman *et al.*, 2021). It was found that the interactions occur almost exclusively through H$\cdots$H contacts, as is typical for van der Waals interactions (Fig. 2). A small fraction is also due to H$\cdots$F interactions. Interactions *via* the N atoms or the B atom do not take place. A decomposition of the interaction energy between the molecules reveals that the interaction is predominantly mediated by dispersion forces, with electrostatic or polarization components being negligible (Fig. 3).

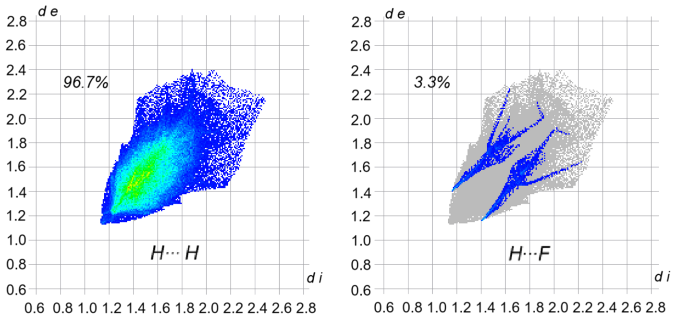

Figure 2
Decomposed two-dimensional fingerprint plots of the interactions of compound **1** devided in reciprocal H$\cdots$H (left) and H$\cdots$F (right) contacts along with their contributions (*CrystalExplorer*; Spackman *et al.*, 2021).

4. Database survey

A database search [Cambridge Structural Database (CSD), Version 5.45, update June 2024; Groom *et al.*, 2016] for analogous compounds reveals only two diaminofluoroboranes with acyclic amines (CSD refcodes YUBMUE and YUBNEP; Ott *et al.*, 2009). The major difference between these compounds and compound **1** is that only one of the amines has two isopropyl substituents, while the other amine is substituted with an aromatic substituent and a proton. The B—F bond lengths in both structures range from 1.363 to 1.368 Å, the B—N bonds to the isopropyl-substituted amines range from 1.395 to 1.410 Å and the N—B—N bond angles range from 126.90 to 128.21°. Furthermore, an expanded search, encompassing diisopropylamine-substituted trigonal–planar boranes in general, yields 351 entries, with the B—N bond lengths ranging from 1.316 to 1.501 Å, contingent on the specific substituents on the B atom. Subsequent to quaternization of the N atom by protonation, a substantial elongation of the B—N bond is observed (1.571 Å in YUBNOZ; Ott *et al.*, 2009), attributable to the elimination of the partial double-bond character.

5. Synthesis and crystallization

5.1. General considerations

All reagents were purchased from commercial suppliers and used without further purification. Pentane was dried using lithium aluminium hydride and distilled before use. Reactions of the air-sensitive compounds were carried out under an inert argon atmosphere using the Schlenk line technique. NMR spectra were recorded on a Bruker Avance (Neo) 500 instruments. NMR spectra were referenced to residual solvent peaks (C_6D_6). Mass spectra were recorded on a Bruker Impact II instrument. The single-crystal X-ray diffraction (SC-XRD) data were collected on a Bruker Venture with a Photon III CMOS detector with Mo $K\alpha$ radiation (λ = 0.71073 Å). The experimental procedure was adapted from Major *et al.* (2019).

5.2. Experimental procedure

Boron trifluoride diethyl etherate (1.63 ml, 13.0 mmol) was dissolved in pentane (50 ml) and the solution cooled to 195 K.

Table 1
Experimental details.

Crystal data	
Chemical formula	$C_{12}H_{28}BFN_2$
M_r	230.17
Crystal system, space group	Triclinic, $P\bar{1}$
Temperature (K)	100
a, b, c (Å)	6.3603 (2), 7.6440 (3), 16.4098 (6)
α, β, γ (°)	84.334 (1), 84.820 (1), 67.518 (1)
V (Å^3)	732.38 (5)
Z	2
Radiation type	Mo $K\alpha$
μ (mm^{-1})	0.07
Crystal size (mm)	0.50 × 0.50 × 0.10
Data collection	
Diffractometer	Bruker D8 VENTURE with a PHOTON III CMOS detector
Absorption correction	Empirical (using intensity measurements) (*SADABS*; Bruker, 2021)
T_{min}, T_{max}	0.514, 0.746
No. of measured, independent and observed [$I > 2\sigma(I)$] reflections	44165, 4103, 3776
R_{int}	0.043
$(\sin \theta/\lambda)_{max}$ (Å^{-1})	0.695
Refinement	
$R[F^2 > 2\sigma(F^2)]$, $wR(F^2)$, S	0.042, 0.110, 1.08
No. of reflections	4103
No. of parameters	153
H-atom treatment	H-atom parameters constrained
$\Delta\rho_{max}$, $\Delta\rho_{min}$ (e Å^{-3})	0.51, −0.27

Computer programs: *SAINT-Plus* (Bruker, 2021), SHELXT2018 (Sheldrick, 2015*a*), *SHELXL2019* (Lübben *et al.*, 2019; Sheldrick, 2015*b*), *SHELXTL* (Sheldrick, 2008), *APEX4* (Bruker, 2021) and *publCIF* (Westrip, 2010).

A solution of lithium diisopropylamide in THF (13.0 ml, 26.0 mmol, 2 *M*) was then added dropwise. The resulting solution was stirred for 7 h at 195 K and then for 14 h at room temperature. A precipitated orange solid was separated by filtration and the resulting solution was concentrated *in vacuo* at 273 K. The residue was redissolved in *n*-pentane (7 ml) and stored at 247 K for 2 d. The suspension was then cooled to 195 K and the precipitated yellowish solid was separated by filtration. The solvent was removed *in vacuo* and the uptake in pentane and subsequent filtration were repeated as described above. Compound **1** was obtained as a yellowish crystalline solid (yield: 1.13 g, 4.91 mmol). Colourless crystals suitable for X-ray crystallography were obtained from the solid by sublimation (yield 38%). ^{1}H NMR (500 MHz, C_6D_6): δ (ppm) 3.20 [hept, $^3J_{HH} = 6.7$ Hz, 4H, NC*H*(CH$_3$)$_2$], 1.18 [*d*, $^3J_{HH} = 6.9$ Hz, 24H, NCH(C*H*$_3$)$_2$]. ^{13}C{^{1}H} NMR (101 MHz, C_6D_6): δ (ppm) 45.3 [*N*CH(CH$_3$)$_2$], 23.9 [*d*, $^4J_{CF} = 2.5$ Hz, NCH(*C*H$_3$)$_2$]. ^{11}B {^{1}H} NMR (160 MHz, C_6D_6): δ (ppm) 25.0 (*s*). ^{19}F{^{1}H} NMR (471 MHz, C_6D_6): δ (ppm) −108.9 (*s*).

6. Refinement

Crystal data, data collection and structure refinement details are summarized in Table 1. H atoms were placed at ideal calculated positions and refined using a riding model.

Acknowledgements

The authors would like to acknowledge Professor Jens Müller for financial and non-material support, as well as for providing access to laboratories and chemicals. MH would like to thank the funds of the chemical industry (VCI) for their support.

References

Bruker (2021). *APEX4*, *SAINT-Plus* and *SADABS*. Bruker AXS Inc., Madison, Wisconsin, USA.

Edwards, I. A. S. & Stadler, H. P. (1970). *Acta Cryst.* B**26**, 1905–1908.

Groom, C. R., Bruno, I. J., Lightfoot, M. P. & Ward, S. C. (2016). *Acta Cryst.* B**72**, 171–179.

Hazell, A. C. (1966). *J. Chem. Soc. A*, pp. 1392–1394.

Higashi, J., Eastman, A. D. & Parry, R. W. (1982). *Inorg. Chem.* **21**, 716–720.

Jones, P. G. (1984). *Acta Cryst.* C**40**, 1465–1466.

Kölle, P. & Nöth, H. (1986). *Chem. Ber.* **119**, 313–324.

Lübben, J., Wandtke, C. M., Hübschle, C. B., Ruf, M., Sheldrick, G. M. & Dittrich, B. (2019). *Acta Cryst.* A**75**, 50–62.

Major, C. J., Bamford, K. L., Qu, Z.-W. & Stephan, D. W. (2019). *Chem. Commun.* **55**, 5155–5158.

Maringgele, W., Meller, A., Dielkus, S. & Herbst-Irmer, R. (1993). *Z. Naturforsch. B*, **48**, 561–570.

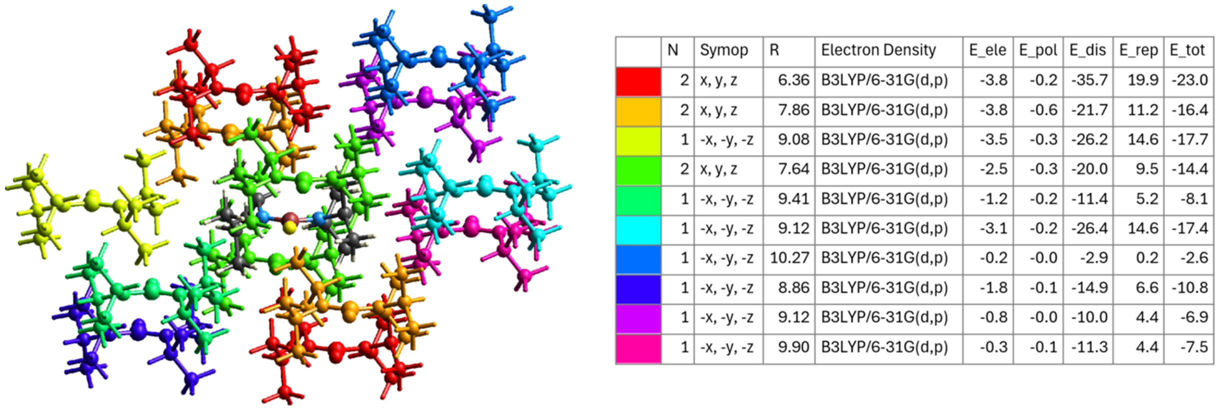

	N	Symop	R	Electron Density	E_ele	E_pol	E_dis	E_rep	E_tot
🟥	2	x, y, z	6.36	B3LYP/6-31G(d,p)	-3.8	-0.2	-35.7	19.9	-23.0
🟧	2	x, y, z	7.86	B3LYP/6-31G(d,p)	-3.8	-0.6	-21.7	11.2	-16.4
🟨	1	-x, -y, -z	9.08	B3LYP/6-31G(d,p)	-3.5	-0.3	-26.2	14.6	-17.7
🟩	2	x, y, z	7.64	B3LYP/6-31G(d,p)	-2.5	-0.3	-20.0	9.5	-14.4
🟩	1	-x, -y, -z	9.41	B3LYP/6-31G(d,p)	-1.2	-0.2	-11.4	5.2	-8.1
🟦	1	-x, -y, -z	9.12	B3LYP/6-31G(d,p)	-3.1	-0.2	-26.4	14.6	-17.4
🟦	1	-x, -y, -z	10.27	B3LYP/6-31G(d,p)	-0.2	-0.0	-2.9	0.2	-2.6
🟦	1	-x, -y, -z	8.86	B3LYP/6-31G(d,p)	-1.8	-0.1	-14.9	6.6	-10.8
🟪	1	-x, -y, -z	9.12	B3LYP/6-31G(d,p)	-0.8	-0.0	-10.0	4.4	-6.9
🟪	1	-x, -y, -z	9.90	B3LYP/6-31G(d,p)	-0.3	-0.1	-11.3	4.4	-7.5

Figure 3
Interaction energies (in kJ mol^{-1}) for different contacts within the structure of **1**, divided into electrostatic, polarization, dispersion and repulsive contributions, together with the total interaction energy. In the partial packing diagram (left), the interacting molecules are colour-coded to correlate with the tabulated energies (*CrystalExplorer*; Spackman *et al.*, 2021).

Maringgele, W., Seebold, U., Meller, A., Dielkus, S., Pohl, E., Herbst–Irmer, R. & Sheldrick, G. M. (1992). *Chem. Ber.* **125**, 1559–1564.

Nöth, H. & Rasthofer, B. (1986). *Chem. Ber.* **119**, 2075–2079.

Nöth, H., Rasthofer, B. & Weber, S. (1984). *Z. Naturforsch B*, **39**, 1058–1068.

Nöth, H., Staudigl, R. & Wagner, H.-U. (1982). *Inorg. Chem.* **21**, 706–716.

Ott, H., Matthes, C., Ringe, A., Magull, J., Stalke, D. & Klingebiel, U. (2009). *Chem. A Eur. J.* **15**, 4602–4609.

Sheldrick, G. M. (2008). *Acta Cryst.* A**64**, 112–122.

Sheldrick, G. M. (2015*a*). *Acta Cryst.* A**71**, 3–8.

Sheldrick, G. M. (2015*b*). *Acta Cryst.* C**71**, 3–8.

Spackman, P. R., Turner, M. J., McKinnon, J. J., Wolff, S. K., Grimwood, D. J., Jayatilaka, D. & Spackman, M. A. (2021). *J. Appl. Cryst.* **54**, 1006–1011.

Westrip, S. P. (2010). *J. Appl. Cryst.* **43**, 920–925.

supporting information

Acta Cryst. (2025). E**81** [https://doi.org/10.1107/S2056989025003160]

Crystal structure of bis(diisopropylamino)fluoroborane

Tabea Lenz and Marian Hebenbrock

Computing details

Bis(diisopropylamino)fluoroborane

Crystal data

$C_{12}H_{28}BFN_2$
$M_r = 230.17$
Triclinic, $P\overline{1}$
$a = 6.3603$ (2) Å
$b = 7.6440$ (3) Å
$c = 16.4098$ (6) Å
$\alpha = 84.334$ (1)°
$\beta = 84.820$ (1)°
$\gamma = 67.518$ (1)°
$V = 732.38$ (5) Å^3

$Z = 2$
$F(000) = 256$
$D_x = 1.044$ Mg m^{-3}
Mo $K\alpha$ radiation, $\lambda = 0.71073$ Å
Cell parameters from 9941 reflections
$\theta = 2.5$–29.6°
$\mu = 0.07$ mm^{-1}
$T = 100$ K
Plate, colourless
0.50 × 0.50 × 0.10 mm

Data collection

Bruker D8 VENTURE with a PHOTON III CMOS detector diffractometer
Radiation source: microsource
f\ and w\ scans
Absorption correction: empirical (using intensity measurements) (SADABS; Bruker, 2021)
$T_{\min} = 0.514$, $T_{\max} = 0.746$

44165 measured reflections
4103 independent reflections
3776 reflections with $I > 2\sigma(I)$
$R_{\text{int}} = 0.043$
$\theta_{\max} = 29.6°$, $\theta_{\min} = 2.5°$
$h = -8\rightarrow8$
$k = -10\rightarrow10$
$l = -22\rightarrow22$

Refinement

Refinement on F^2
Least-squares matrix: full
$R[F^2 > 2\sigma(F^2)] = 0.042$
$wR(F^2) = 0.110$
$S = 1.08$
4103 reflections
153 parameters
0 restraints
Primary atom site location: intrinsic phasing

Hydrogen site location: inferred from neighbouring sites
H-atom parameters constrained
$w = 1/[\sigma^2(F_o^2) + (0.0628P)^2 + 0.1203P]$ where $P = (F_o^2 + 2F_c^2)/3$
$(\Delta/\sigma)_{\max} = 0.001$
$\Delta\rho_{\max} = 0.51$ e Å^{-3}
$\Delta\rho_{\min} = -0.27$ e Å^{-3}

Special details

Geometry. All esds (except the esd in the dihedral angle between two l.s. planes) are estimated using the full covariance matrix. The cell esds are taken into account individually in the estimation of esds in distances, angles and torsion angles; correlations between esds in cell parameters are only used when they are defined by crystal symmetry. An approximate (isotropic) treatment of cell esds is used for estimating esds involving l.s. planes.

Fractional atomic coordinates and isotropic or equivalent isotropic displacement parameters (Å^2)

	x	y	z	$U_{\rm iso}$*/$U_{\rm eq}$
F1	0.93904 (9)	0.04267 (7)	0.71623 (3)	0.02497 (13)
N1	0.88667 (11)	0.25106 (9)	0.81925 (4)	0.01548 (13)
N2	0.72717 (11)	0.36432 (9)	0.67705 (4)	0.01613 (14)
C1	0.94682 (13)	0.09107 (10)	0.88255 (4)	0.01678 (15)
H1	0.948918	0.145510	0.935300	0.020*
C2	1.18385 (14)	−0.06119 (12)	0.86768 (5)	0.02304 (17)
H2A	1.224662	−0.148577	0.916731	0.035*
H2B	1.295300	−0.000875	0.855770	0.035*
H2C	1.183618	−0.131787	0.821000	0.035*
C3	0.76418 (15)	0.00544 (12)	0.89528 (5)	0.02429 (17)
H3A	0.803276	−0.093603	0.940334	0.036*
H3B	0.755731	−0.049951	0.844889	0.036*
H3C	0.616325	0.104925	0.908771	0.036*
C4	0.88051 (12)	0.43069 (10)	0.84597 (4)	0.01606 (15)
H4	0.845794	0.524505	0.797241	0.019*
C5	0.69137 (14)	0.51110 (11)	0.91219 (5)	0.02059 (16)
H5A	0.679720	0.638557	0.922731	0.031*
H5B	0.726963	0.428370	0.962753	0.031*
H5C	0.546150	0.517926	0.893549	0.031*
C6	1.11067 (14)	0.41371 (12)	0.87467 (5)	0.02167 (16)
H6A	1.103194	0.539362	0.886261	0.033*
H6B	1.229965	0.362372	0.831561	0.033*
H6C	1.146032	0.328549	0.924554	0.033*
C7	0.54639 (12)	0.54721 (10)	0.69565 (4)	0.01650 (15)
H7	0.528695	0.550183	0.756731	0.020*
C8	0.60564 (14)	0.71800 (11)	0.66229 (5)	0.02176 (16)
H8A	0.486698	0.834686	0.681208	0.033*
H8B	0.615843	0.724314	0.602201	0.033*
H8C	0.752295	0.704329	0.682121	0.033*
C9	0.31532 (13)	0.56770 (12)	0.66626 (5)	0.02146 (16)
H9A	0.197235	0.685037	0.684966	0.032*
H9B	0.277831	0.458913	0.688826	0.032*
H9C	0.323321	0.572230	0.606207	0.032*
C10	0.76673 (13)	0.32376 (11)	0.58934 (4)	0.01805 (15)
H10	0.680044	0.444801	0.557470	0.022*
C11	1.01744 (15)	0.26992 (13)	0.56098 (5)	0.02464 (17)
H11A	1.036191	0.253792	0.501909	0.037*
H11B	1.108985	0.150774	0.590426	0.037*
H11C	1.068066	0.370637	0.572384	0.037*
C12	0.67586 (15)	0.17610 (13)	0.56824 (5)	0.02438 (17)
H12A	0.687330	0.168847	0.508612	0.037*
H12B	0.516015	0.212989	0.588332	0.037*
H12C	0.766010	0.051867	0.594240	0.037*
B1	0.84742 (14)	0.22573 (12)	0.73804 (5)	0.01686 (16)

Atomic displacement parameters (Å^2)

	U^{11}	U^{22}	U^{33}	U^{12}	U^{13}	U^{23}
F1	0.0343 (3)	0.0151 (2)	0.0207 (2)	−0.0022 (2)	−0.00725 (19)	−0.00367 (17)
N1	0.0176 (3)	0.0128 (3)	0.0152 (3)	−0.0044 (2)	−0.0035 (2)	0.0002 (2)
N2	0.0178 (3)	0.0154 (3)	0.0136 (3)	−0.0040 (2)	−0.0021 (2)	−0.0016 (2)
C1	0.0178 (3)	0.0150 (3)	0.0164 (3)	−0.0050 (3)	−0.0036 (2)	0.0015 (2)
C2	0.0202 (4)	0.0188 (4)	0.0247 (4)	−0.0013 (3)	−0.0048 (3)	0.0011 (3)
C3	0.0249 (4)	0.0237 (4)	0.0270 (4)	−0.0130 (3)	−0.0048 (3)	0.0047 (3)
C4	0.0170 (3)	0.0150 (3)	0.0168 (3)	−0.0064 (3)	−0.0035 (2)	−0.0003 (2)
C5	0.0210 (4)	0.0187 (3)	0.0206 (3)	−0.0051 (3)	−0.0014 (3)	−0.0046 (3)
C6	0.0208 (4)	0.0244 (4)	0.0233 (4)	−0.0120 (3)	−0.0062 (3)	0.0016 (3)
C7	0.0162 (3)	0.0157 (3)	0.0161 (3)	−0.0040 (3)	−0.0025 (2)	−0.0007 (2)
C8	0.0245 (4)	0.0174 (3)	0.0230 (4)	−0.0074 (3)	−0.0045 (3)	0.0015 (3)
C9	0.0173 (3)	0.0250 (4)	0.0210 (3)	−0.0063 (3)	−0.0034 (3)	−0.0012 (3)
C10	0.0204 (3)	0.0195 (3)	0.0137 (3)	−0.0065 (3)	−0.0022 (2)	−0.0017 (2)
C11	0.0224 (4)	0.0285 (4)	0.0217 (4)	−0.0083 (3)	0.0026 (3)	−0.0047 (3)
C12	0.0296 (4)	0.0261 (4)	0.0206 (4)	−0.0125 (3)	−0.0046 (3)	−0.0049 (3)
B1	0.0179 (4)	0.0151 (4)	0.0166 (3)	−0.0048 (3)	−0.0022 (3)	−0.0015 (3)

Geometric parameters (Å, º)

F1—B1	1.3650 (9)	C6—H6A	0.9800
N1—B1	1.4227 (10)	C6—H6B	0.9800
N1—C4	1.4676 (9)	C6—H6C	0.9800
N1—C1	1.4779 (9)	C7—C8	1.5310 (11)
N2—B1	1.4206 (10)	C7—C9	1.5343 (10)
N2—C7	1.4701 (9)	C7—H7	1.0000
N2—C10	1.4812 (9)	C8—H8A	0.9800
C1—C3	1.5272 (11)	C8—H8B	0.9800
C1—C2	1.5280 (11)	C8—H8C	0.9800
C1—H1	1.0000	C9—H9A	0.9800
C2—H2A	0.9800	C9—H9B	0.9800
C2—H2B	0.9800	C9—H9C	0.9800
C2—H2C	0.9800	C10—C11	1.5266 (11)
C3—H3A	0.9800	C10—C12	1.5298 (11)
C3—H3B	0.9800	C10—H10	1.0000
C3—H3C	0.9800	C11—H11A	0.9800
C4—C5	1.5284 (11)	C11—H11B	0.9800
C4—C6	1.5326 (10)	C11—H11C	0.9800
C4—H4	1.0000	C12—H12A	0.9800
C5—H5A	0.9800	C12—H12B	0.9800
C5—H5B	0.9800	C12—H12C	0.9800
C5—H5C	0.9800		

B1—N1—C4	123.84 (6)	H6B—C6—H6C	109.5
B1—N1—C1	121.01 (6)	N2—C7—C8	113.11 (6)
C4—N1—C1	115.11 (6)	N2—C7—C9	112.27 (6)

B1—N2—C7	123.64 (6)	C8—C7—C9	110.19 (6)
B1—N2—C10	120.53 (6)	N2—C7—H7	107.0
C7—N2—C10	115.66 (6)	C8—C7—H7	107.0
N1—C1—C3	111.48 (6)	C9—C7—H7	107.0
N1—C1—C2	113.89 (6)	C7—C8—H8A	109.5
C3—C1—C2	111.49 (7)	C7—C8—H8B	109.5
N1—C1—H1	106.5	H8A—C8—H8B	109.5
C3—C1—H1	106.5	C7—C8—H8C	109.5
C2—C1—H1	106.5	H8A—C8—H8C	109.5
C1—C2—H2A	109.5	H8B—C8—H8C	109.5
C1—C2—H2B	109.5	C7—C9—H9A	109.5
H2A—C2—H2B	109.5	C7—C9—H9B	109.5
C1—C2—H2C	109.5	H9A—C9—H9B	109.5
H2A—C2—H2C	109.5	C7—C9—H9C	109.5
H2B—C2—H2C	109.5	H9A—C9—H9C	109.5
C1—C3—H3A	109.5	H9B—C9—H9C	109.5
C1—C3—H3B	109.5	N2—C10—C11	111.40 (6)
H3A—C3—H3B	109.5	N2—C10—C12	113.43 (6)
C1—C3—H3C	109.5	C11—C10—C12	111.42 (7)
H3A—C3—H3C	109.5	N2—C10—H10	106.7
H3B—C3—H3C	109.5	C11—C10—H10	106.7
N1—C4—C5	112.25 (6)	C12—C10—H10	106.7
N1—C4—C6	112.37 (6)	C10—C11—H11A	109.5
C5—C4—C6	110.44 (6)	C10—C11—H11B	109.5
N1—C4—H4	107.2	H11A—C11—H11B	109.5
C5—C4—H4	107.2	C10—C11—H11C	109.5
C6—C4—H4	107.2	H11A—C11—H11C	109.5
C4—C5—H5A	109.5	H11B—C11—H11C	109.5
C4—C5—H5B	109.5	C10—C12—H12A	109.5
H5A—C5—H5B	109.5	C10—C12—H12B	109.5
C4—C5—H5C	109.5	H12A—C12—H12B	109.5
H5A—C5—H5C	109.5	C10—C12—H12C	109.5
H5B—C5—H5C	109.5	H12A—C12—H12C	109.5
C4—C6—H6A	109.5	H12B—C12—H12C	109.5
C4—C6—H6B	109.5	F1—B1—N2	116.05 (7)
H6A—C6—H6B	109.5	F1—B1—N1	115.03 (6)
C4—C6—H6C	109.5	N2—B1—N1	128.91 (7)
H6A—C6—H6C	109.5		

B1—N1—C1—C3	−58.17 (9)	B1—N2—C10—C11	−57.08 (9)
C4—N1—C1—C3	124.16 (7)	C7—N2—C10—C11	127.52 (7)
B1—N1—C1—C2	69.05 (9)	B1—N2—C10—C12	69.60 (9)
C4—N1—C1—C2	−108.62 (7)	C7—N2—C10—C12	−105.80 (8)
B1—N1—C4—C5	117.02 (8)	C7—N2—B1—F1	154.87 (7)
C1—N1—C4—C5	−65.38 (8)	C10—N2—B1—F1	−20.15 (10)
B1—N1—C4—C6	−117.78 (8)	C7—N2—B1—N1	−25.31 (12)
C1—N1—C4—C6	59.82 (8)	C10—N2—B1—N1	159.67 (8)
B1—N2—C7—C8	117.08 (8)	C4—N1—B1—F1	156.92 (7)

C10—N2—C7—C8	−67.68 (8)	C1—N1—B1—F1	−20.55 (10)
B1—N2—C7—C9	−117.45 (8)	C4—N1—B1—N2	−22.91 (12)
C10—N2—C7—C9	57.79 (8)	C1—N1—B1—N2	159.63 (7)